e-ISSN: 2250-0758 | p-ISSN: 2394-6962
Volume-12, Issue-4 (August 2022)
https://doi.org/10.31033/ijemr.12.4.27

Effect of Pulsating Current on 304HCU GTAW Joints

Tushar Singh Tomar
B. Tech., Mechanical Engineering, S. R. M. Institute of Science & Technology, Kattankulathur, Chennai, Tamil Nadu, INDIA

ABSTRACT

Super 304HCu super austenitic stainless-steel tubes containing 2.3 to 3 (Wt.%) Copper (Cu) are used in high temperature tubes and reheating of nuclear power plants. In general, stainless steel austenitic welded by conventional gas tungsten arc welding (CC-GTAW) now produces solid column grains, alloy disintegration and may result in lower mechanical properties. Pulsed current gas tungsten arc welding (PCGTAW) can control the formation of solids by altering the existing gradients in the weld.

Super 304HCu OD 60.5 mm tubes and 3.5 mm wall thickness are automatically welded using CC and PC-GTAW processes. The joints can be detected using optical microscopy, a robust machine and a Vickers microhardness tester. The thermal properties of weld joints were tested and associated with their sub-structural features.

***Keywords*—** Pulsating, PCGTAW, Pipes

I. OBJECTIVES AND METHODOLOGY

Objectives

- The behavior of 304HCu weld joints under the effect of pulsating current (CC-GTAW & PC-GTAW).
- Measure the deformation stress and strain on the material.
- Comparison of the deformative properties and effect of pulsating current on 304 SS and 304Hcu.

Methodology

The material was obtained from Paris corner, Chennai and the pipe was divided into 6 parts at the same place. The welding was done at Guindy, Chennai into four pairs – 2 CCGTAW and 2PCGTAW. The sample cutting was done at Marailmalai Nagar, Kattankulathur. 3 sets of samples were procured. Testing was done at SRMIST-KTR and VIT Chennai. 4 test were conducted.

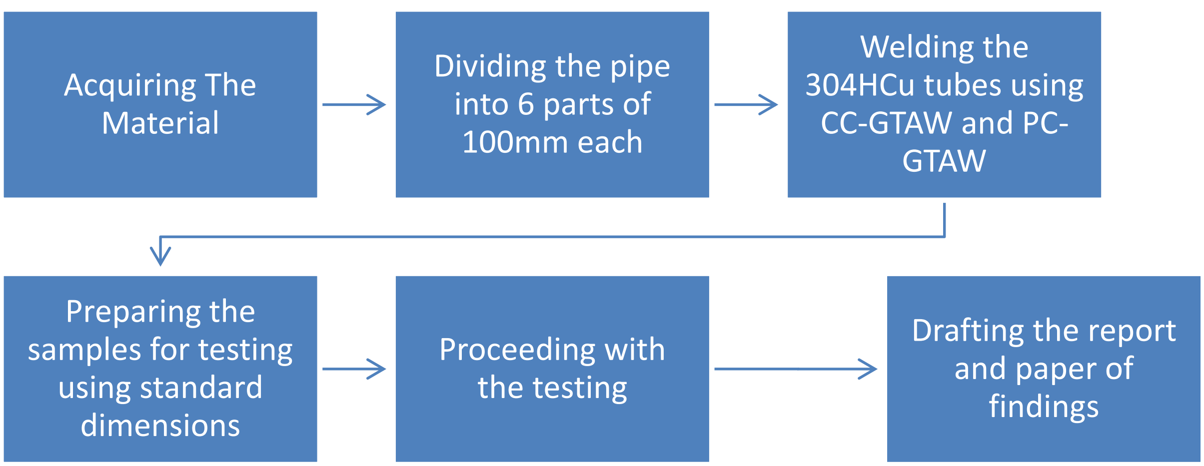

II. EXPERIMENTAL INVESTIGATIONS AND RESULTS

Experimental Investigations

Material:

Figures 4.1 & 4.2 provide us with Side-view and Top-view of the 100mm pipes that were used for the experiment. This result was arranged from a 600mm pipe that was cut into 6 equal parts of 100mm each. The dimensions of the pipes are:

1.) Outer Diameter - 60.5 mm
2.) Length – 100mm
3.) Thickness – 3.5 mm

e-ISSN: 2250-0758 | p-ISSN: 2394-6962
Volume-12, Issue-4 (August 2022)
https://doi.org/10.31033/ijemr.12.4.27


FIG 4.1 SIDE-VIEW

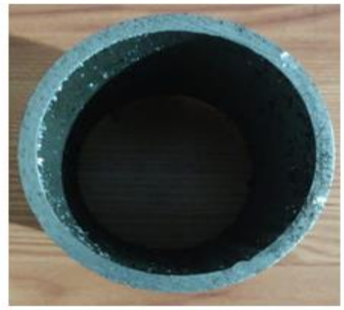
FIG 4.2 TOP-VIEW

Table 4.1 gives the values for the general properties for the material. The table indicated the laboratory tested values for the material SS 304HCu. On comparison with normal grade 304 SS, we can find differences that make 304HCu grade better. The ultimate Tensile Strength for the grade 304SS is around 500 – 600 MPa while for SS 304HCu it exceeds 600 MPa. The %Elongation for 304 SS is less than 40% whereas 304HCu has this value over 43%. These properties indicate that as just a base material, SS 304HCu outperforms the normal grade steel.

TABLE 4.1: General Properties For The Material

Material	**SS304HCu**
UTS (MPa)	613
YS (MPa)	308
%Elongation	43.2%
Density (g/cm^3)	8.03

Table 4.2 gives the chemical composition of the material. This gives in detail explanation as to what differentiates 304HCu grade from normal grade. The presence of copper with over 3wt% and chromium over 18wt% makes it much more reliable than normal grade.

TABLE 4.2: Chemical Composition (WT. %) of 304HCU Super Ass Tube

C	Si	Mn	P	S	Cr	Ni	N	Cu	Nb	B	Al
0.086	0.23	0.81	0.021	0.0003	18.18	9.06	0.095	3.080	0.045	0.0039	0.01

Preparation Of The Specimen Welding


FIG 4.3 WELDING SETUP


FIG 4.4 CC-GTAW


FIG 4.5 PC-GTAW

e-ISSN: 2250-0758 | p-ISSN: 2394-6962
Volume-12, Issue-4 (August 2022)
https://doi.org/10.31033/ijemr.12.4.27

The Welding was carried out at Arun technologies, arumbakkam. The two types of welding done can be seen in the figure 4.4 and figure 4.5. The joints were welded using CCGTAW and PCGTAW with argon as the shielding gas to prevent oxidation of the weld. The welding parameters used in this investigation are shown in Table 4.3. CC- GTAW had a direct output whereas PC-GTAW had a constant pulse running through with visible intensity peaks.

TABLE 4.3: Welding Parameters Used In This Investigation

Parameters	CC - GTAW	PC - GTAW
Peak Current(A)	-	110
Base Current(A)	-	66
% on time	-	75
Frequency (Hz)	-	10
Current(A)	100	-
Voltage(V)	11	11
Welding Speed (mm/m in)	70	70
Heat Input(kJ/mm)	0.943	0.933

Table 4.3 shows us the difference in weld parameters for CCGTAW and PCGTAW. From the CCGTAW column we can observe that there is no peak or base current, just a fixed value that runs throughout the process whereas from the PCGTAW column we can observe the fact that there is a peak and base current with a certain frequency. This denotes the fact that pulses are used in PCGTAW and there is a peak current and cooling time which allows for better grain refinement.

Samples

Samples were cut according to the following:

1.) Tensile Test – Standard Size (Figure 4.11)
2.) Microstructure – 10 mm x 10mm
3.) Microhardness – 10 mm x 10mm
4.) XRD – 1 mm x 10mm

(Thickness of all being the same as that of the pipes)

e-ISSN: 2250-0758 | p-ISSN: 2394-6962
Volume-12, Issue-4 (August 2022)
https://doi.org/10.31033/ijemr.12.4.27

Fig 4.6 CC-GTAW PIPE

Fig 4.7 PC-GTAW PIPE

Figures 4.6 and 4.7 shows the prepared samples for CC-GTAW and PC-GTAW respectively for two 100mm pipes joined together to produce one sample each for both types of welds.

Fig 4.8 ORIGINAL MATERIAL SAMPLES

Fig 4.9 CC-GTAW SAMPLES

Fig 4.10 PC-GTAW SAMPLES

Figures 4.8, 4.9 & 4.10 shows the samples cut from original material, CC-GTAW joint & PC-GTAW joint respectively, through wire cut electric discharge machining. This was conducted at Om-Shakti Industries in Maraimalai Nagar. The Four samples are in the order as mentioned before with the given dimensions.

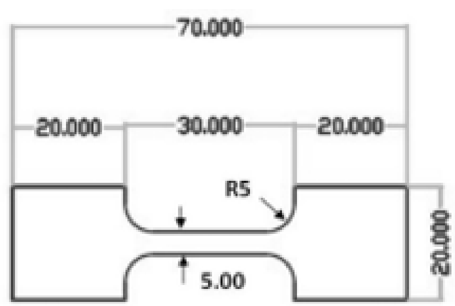

FIG 4.11 STANDARD SIZE FOR TENSILE TEST SAMPLE

e-ISSN: 2250-0758 | p-ISSN: 2394-6962
Volume-12, Issue-4 (August 2022)
https://doi.org/10.31033/ijemr.12.4.27

With the samples now obtained, testing was carried out for all the different samples accordingly.

EXPERIMENTS TO BE CONDUCTED

A total of Four tests were to be conducted on the respective four samples that were prepared.

1.) **TENSILE TEST:**
The tensile test was conducted on sample no. 1 for all the three arrangements – PC-GTAW sample, CC-GTAW sample and Original Sample.
CONDUCTED AT: VIT CHENNAI
COST: Rs. 450/- PER SAMPLE
REQUIRED SPECIFICATIONS:
NOMINAL STRAIN RATE: 1 x 10^{-3} s^{-1}
FEED RATE: 2 mm/min

2.) **MICROSTRUCTURE:**
The microstructure test was carried out on sample no. 2 for all the three arrangements – PC-GTAW sample, CC-GTAW sample and Original Sample.
CONDUCTED AT: SRMIST-KTR
COST: Rs. 250/- PER SAMPLE
REQUIRED SPECIFICATIONS:
EQUIPMENT: OPTICAL MICROSCOPE
MAGNIFICATIONS: 50x AND 100x

3.) **MICROHARDNESS:**
The microhardness test was carried out on sample no. 3 for all the three arrangements – PC-GTAW sample, CC-GTAW sample and Original Sample.
CONDUCTED AT: OMEGA LABS
COST: Rs. 550/- PER SAMPLE
REQUIRED SPECIFICATIONS:
EQUIPMENT: VICKERS MICROHARDNESS TESTER
LOAD: 500g
DWELL TIME: 15s

4.) **X-RAY DIFFRACTION:**
The XRD test was carried out on sample no. 4 for all the three arrangements – PC-GTAW sample, CC-GTAW sample and Original Sample.
CONDUCTED AT: SRMIST-KTR
COST: Rs. 150/- PER SAMPLE

Results:

Tensile Test:

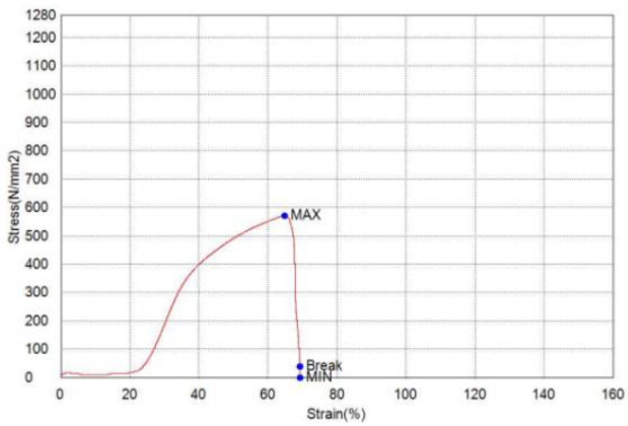

FIG 4.12 STRESS vs STRAIN - PCGTAW

Figure 4.12 shows the trends in stress vs strain results for PCGTAW joint. The elastic limit is at around 350 N/mm^2 after which it proceeds to its maximum tensile limit before reaching the breaking point.

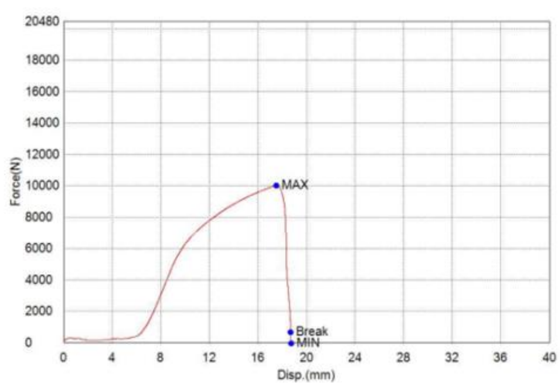

FIG 4.13 FORCE vs DISPLACEMENT - PCGTAW

e-ISSN: 2250-0758 | p-ISSN: 2394-6962
Volume-12, Issue-4 (August 2022)
www.ijemr.net
https://doi.org/10.31033/ijemr.12.4.27

Figure 4.13 shows the trends in force vs displacement results for PCGTAW joint. This indicates the elongation that the material will go through at a certain load.

Table 4.4 gives more detailed values of the results. The maximum force that the PCGTAW joint can withstand is just under 10000 N and it can bear a maximum stress of over 550 N/mm^2.

Table 4.4: PCGTAW Tensile Test Results

Max Force (N)	Max Stress (N/mm^2)	Max Displacement (mm)	Max Strain (%)
9988.57	**570.776**	**17.5209**	**64.8923**

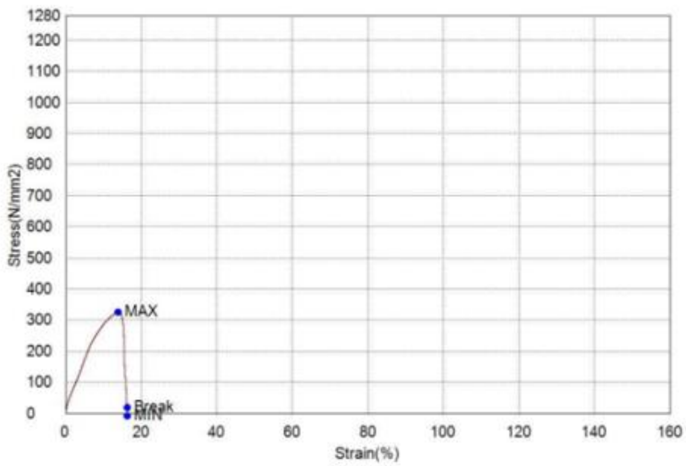

FIG 4.14 STRESS vs STRAIN - CCGTAW

Figure 4.14 shows the trends in stress vs strain results for CCGTAW joint. The elastic limit is at around 150 N/mm^2 after which it proceeds to its maximum tensile limit before reaching the breaking point.

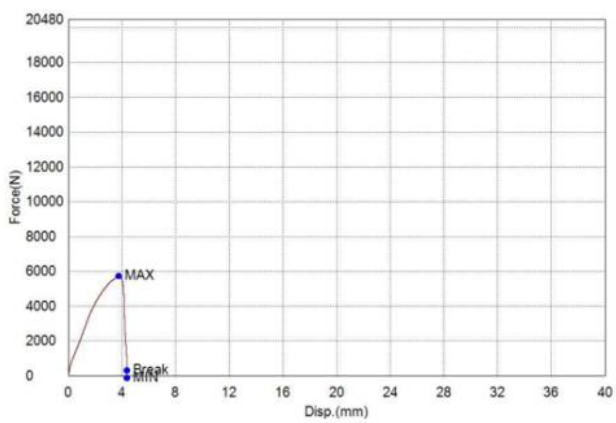

FIG 4.15 FORCE vs DISPLACEMENT - CCGTAW

Figure 4.15 shows the trends in force vs displacement results for CCGTAW joint. This indicates the elongation that the material will go through at a certain load.

Table 4.5 gives more detailed values of the results. The maximum force that the CCGTAW joint can withstand is just over 5700 N and it can bear a maximum stress of over 300 N/mm^2.

e-ISSN: 2250-0758 | p-ISSN: 2394-6962
Volume-12, Issue-4 (August 2022)
https://doi.org/10.31033/ijemr.12.4.27

Table 4.5: CCGTAW Tensile Test Results

Max Force (N)	Max Stress (N/mm^2)	Max Displacement (mm)	Max Strain (%)
5715.14	**326.579**	**3.78158**	**14.0059**

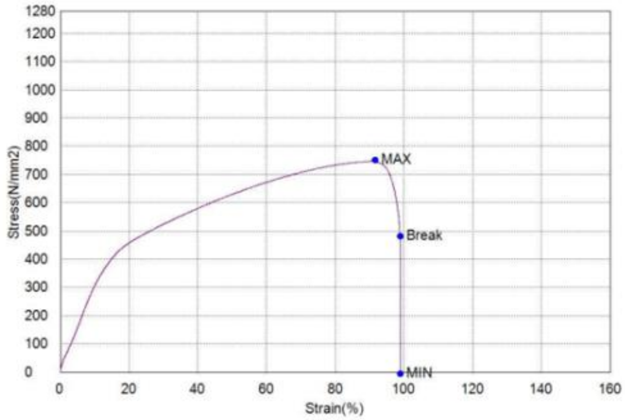

FIG 4.16 STRESS vs STRAIN - ORIGINAL

Figure 4.16 shows the trends in stress vs strain results for original material. The elastic limit is at around 450 N/mm^2 after which it proceeds to its maximum tensile limit before reaching the breaking point.

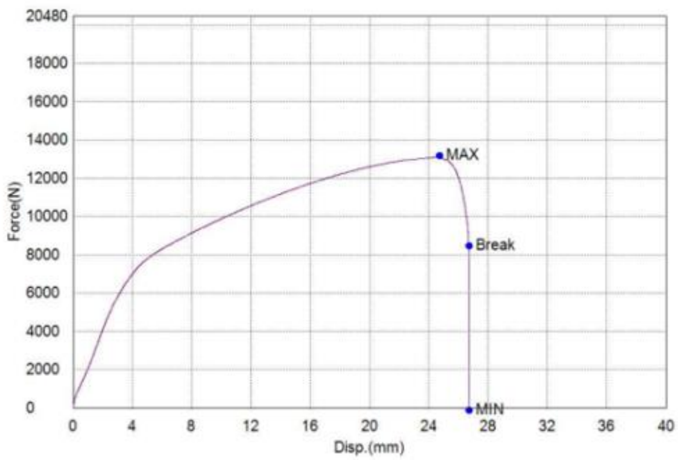

FIG 4.17 FORCE vs DISPLACEMENT - ORIGINAL

Figure 4.17 shows the trends in force vs displacement results for original material. This indicates the elongation that the material will go through at a certain load.

Table 4.6 gives more detailed values of the results. The maximum force that the original material can withstand is over 13000 N and it can bear a maximum stress of over 700 N/mm^2.

Table 4.6: Original Material Tensile Test Results

Max Force (N)	Max Stress (N/mm^2)	Max Displacement (mm)	Max Strain (%)
13161.0	**752.059**	**24.7343**	**91.6083**

e-ISSN: 2250-0758 | p-ISSN: 2394-6962
Volume-12, Issue-4 (August 2022)
https://doi.org/10.31033/ijemr.12.4.27

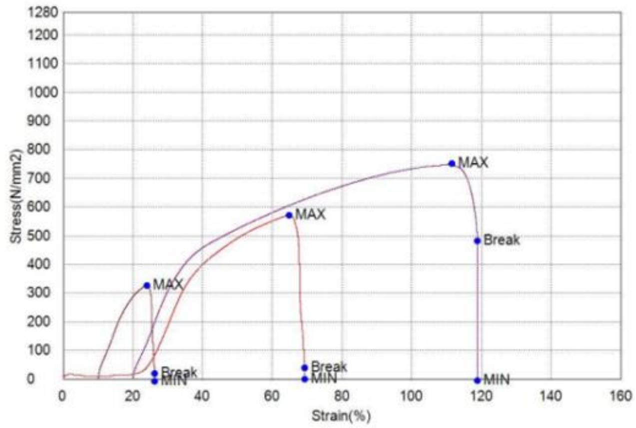

FIG 4.18 STRESS vs STRAIN - COMPARISON

Figure 4.18 displays the comparison among all the three sample results for stress vs strain to give a clearer picture of the samples stand against each other under certain stress.

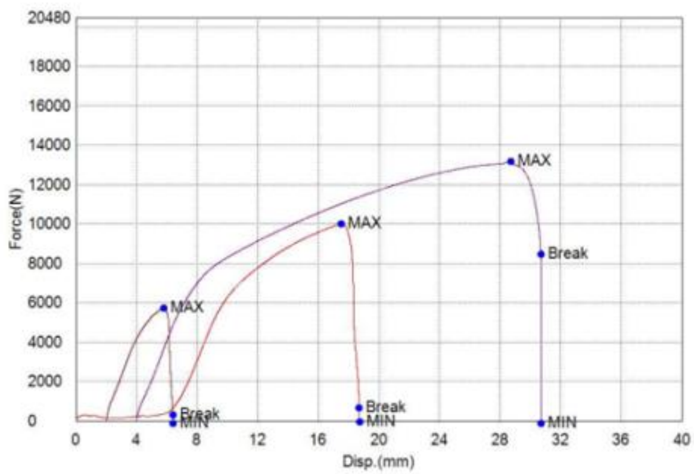

FIG 4.19 FORCE vs DISPLACEMENT - COMPARISON

Figure 4.19 shows the trends in force vs displacement results as a COMPARISON for all the three results.

Table 4.7 gives more detailed values of the results.

Table 4.7: Comparison Of Tensile Test Results

Max Force (N)	Max Stress (N/mm^2)	Max Displacement (mm)	Max Strain (%)
9988.57	**570.776**	**17.5209**	**64.8923**
5715.14	**326.579**	**3.78158**	**14.0059**
13161.0	**752.059**	**24.7343**	**91.6083**

From the final comparison results we can conclude that the PCGTAW joint provides better strength and resistance than the CCGTAW joint. The large difference between the two results further suggests the durability and effectiveness of using the PCGTAW in place of CCGTAW for the joints in the pipe. The comparison with the original material suggests us some room of improvement in the weld region but also tells us how effective PCGTAW is by producing results that are very close to the sample that isn't a joint.

e-ISSN: 2250-0758 | p-ISSN: 2394-6962
Volume-12, Issue-4 (August 2022)
https://doi.org/10.31033/ijemr.12.4.27

Microstructure

The Microstructure of both CCGTAW and PCGTAW joints can be seen from figure 4.20 to 4.26. The results were captured through an Optical Microscope on two magnification settings – 50x and 100x. Figures 4.20 and 4.21 shows the Joint Weld centre for the CCGTAW two aforementioned magnification settings whereas figure 4.22 shows the Joint Weld centre for the PCGTAW on 100x. The CCGTAW joint invariably consists of cellular austenite grains, while PCGTAW joint consists of more random austenite grains of both cellular and columnar morphology. The intercellular separation and interdendritic alloy segregation i.e., dark phase of the best eutectic delta ferrite was revealed in both CCGTAW joints and PCGTAW joints. However, the amount of black phase in PCGTAW joints is lower than CCGTAW joints. Figure 4.23 and 4.24 shows the fusion line and Heat-Affected Zone for the CCGTAW on the two aforementioned magnification settings whereas Figure 4.25 and 4.26 shows the fusion line and Heat-Affected Zone for the PCGTAW. The fusion line optical micrograph of the CCGTAW and PC-GTAW joints, which reveals the grain coarsening in the HAZ due to weld thermal cycles. The HAZ width and grain size of PC-GTAW joint are finer than the CC-GTAW joint. The welding metal near the coupling line indicates the solidification in both cases, initiated by epitaxial growth, followed by planar solidification and switching to the cellular mode to the welding centre. The division of interdendritic alloy segregation i.e., the dark phase is small, non-continuous and highly disturbed in the PCGTA weld and then the CCGTA weld.

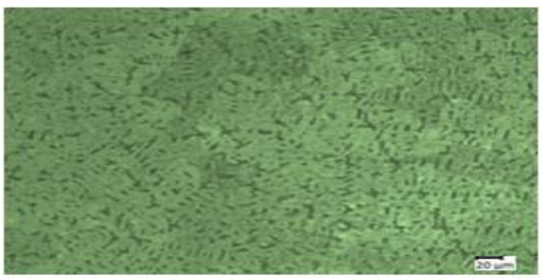

Fig 4.20 CC-GTAW JOINT WELD CENTRE 100X

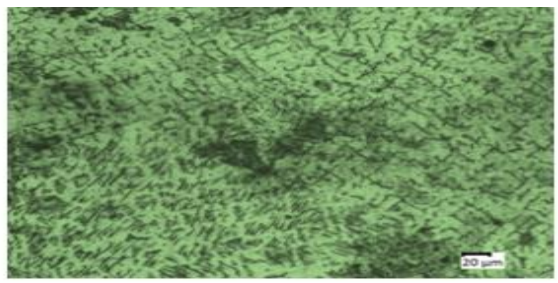

Fig 4.21 CC-GTAW JOINT WELD CENTRE 50X

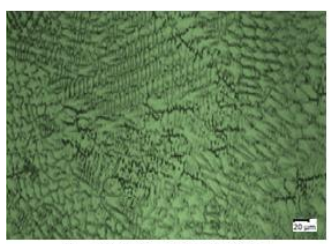

Fig 4.22 PC-GTAW JOINT WELD CENTRE 100X

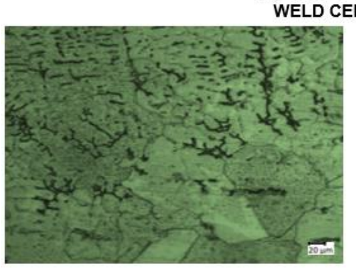

Fig 4.23 CC-GTAW JOINT FUSION LINE 100X

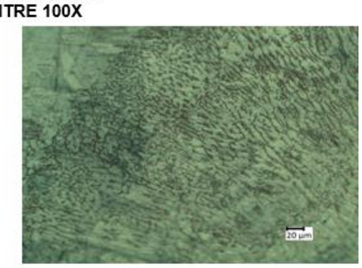

Fig 4.24 CC-GTAW JOINT FUSION LINE 50X

e-ISSN: 2250-0758 | p-ISSN: 2394-6962
Volume-12, Issue-4 (August 2022)
https://doi.org/10.31033/ijemr.12.4.27

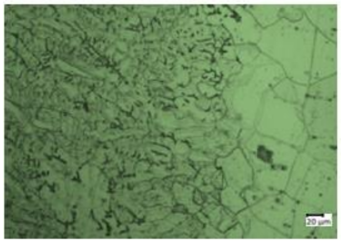

Fig 4.25 PC-GTAW JOINT FUSION LINE 100X

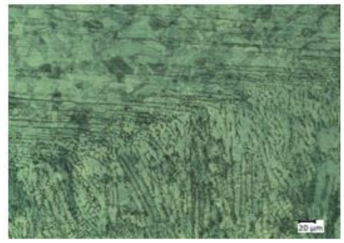

Fig 4.26 PC-GTAW JOINT FUSION LINE 50X

For comparison we can see the microstructure of the original material as well.

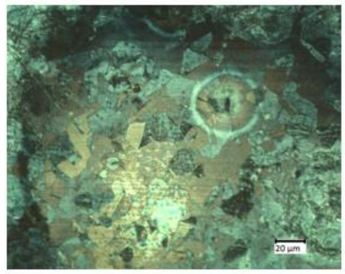

Fig 4.27 OGM 100X

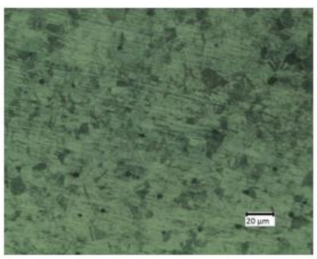

Fig 4.28 OGMS 50X

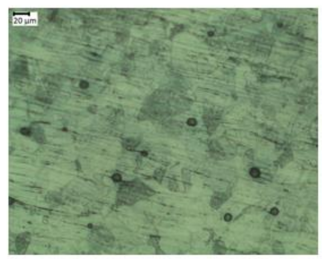

Fig 4.29 OGMS 100X

In figure 4.27 we can see the original material at 100x magnification. We can clearly see a brown material which is copper is large amounts.

Figure 4.28 and 4.29 are further optical analysis of the original material at 50x and 100x.

Microhardness

Hardness measurement was performed using a Vickers microhardness tester with a load of 500 g and a dwell time of 15 s.The microhardness profile of the CCGTAW and PCGTAW joints throughout the weld centreline is shown in Figure 4.30.The lowest strength in the corresponding profile of CCGTAW (146 HV) and PCGTAW (151 HV) was recorded in place of the welding metal joints. The welding centre and HAZ joint of the PCGTAW joint showed higher hardness than CCGTAW joint.

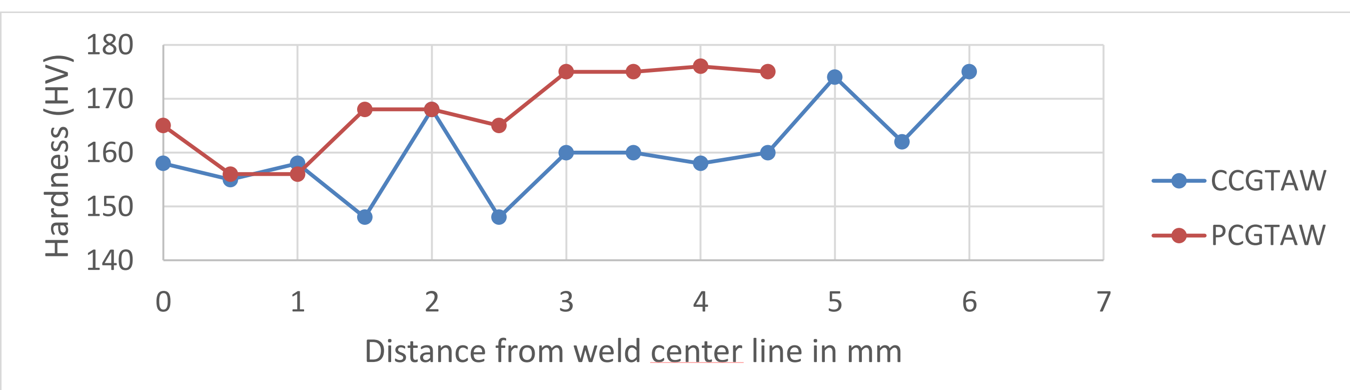

e-ISSN: 2250-0758 | p-ISSN: 2394-6962
Volume-12, Issue-4 (August 2022)
https://doi.org/10.31033/ijemr.12.4.27

Fig 4.30: Hardness (HV) profile across Weld Center Line (WCL)
HAZ for PCGTAW: 2mm – 2.5mm
HAZ for CCGTAW: 3mm – 4mm

X-Ray Diffraction Analysis

The XRD or X-Ray Diffraction test was carried out for all the three samples and the results were analyzed. The analysis of peak profiles for the PCGTAW joint, CCGTAW joint and original material shows the clear difference in the lattice structure. The variation in lattice parameter is studied to understand the influence of deformation on precipitation.

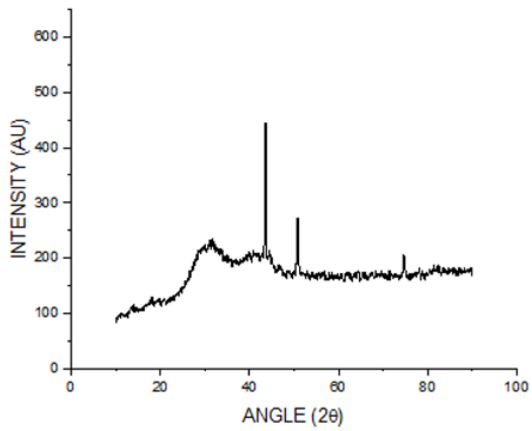

Fig 31: PCGTAW PEAK

Figure 4.31: indicates the peak of crystalline structure of the material after pulsed current TIG welding.

Highest Peak (Intensity): 580
Angle of the Highest Peak: 43.57°

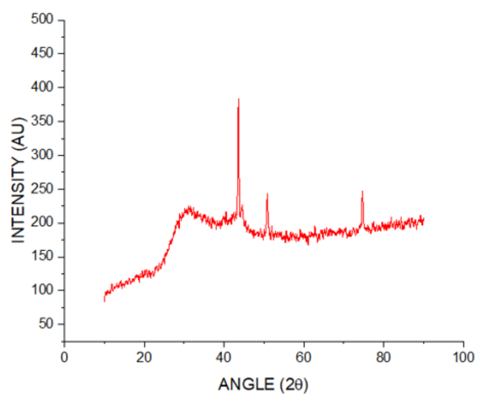

Fig 4.32: CCGTAW PEAK

Figure 4.32: indicates the peak of crystalline structure of the material after constant current TIG welding.
Highest Peak (Intensity): 453
Angle of the Highest Peak: 43.57°

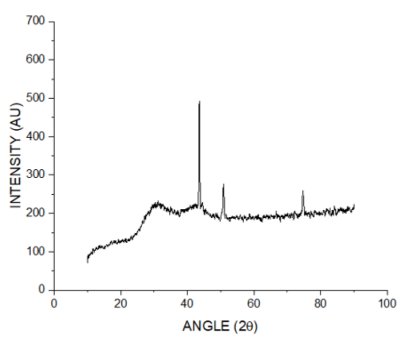

Fig 4.33: ORIGINAL MATERIAL PEAK

Figure 4.33: indicates the peak of crystalline structure of the material after constant current TIG welding.

e-ISSN: 2250-0758 | p-ISSN: 2394-6962
Volume-12, Issue-4 (August 2022)
https://doi.org/10.31033/ijemr.12.4.27

Highest Peak (Intensity): 651
Angle of the Highest Peak: 43.57°

Higher number of peaks indicate a more crystalline structure and as we can make out from the data available that the PCGTAW clearly has a greater number of peaks as well as greater intensity of highest peak than CCGTAW. This entertains the fact that PCGTAW joint is more crystalline in nature thus better at withstanding the deformations and fluctuations than its CCGTAW counterpart.

V. CONCLUSION

The PC-GTAW assembly has shown stronger strength and longer values than CC-GTAW with welding metal failure. The power and length values are reduced by increasing the test temperature in both CCGTAW and PC-GTAW members. Current pulsing resulted in grain refinement, with more high angle grain boundaries in the weld metal The HAZ regions of both CCGTAW and PC-GTAW possess higher hardness than weld metal, due to the highly stable microstructure of the Super 304HCu. When cooled most ferrite remains stable and appears as a continuous component near the boundary. Super 304HCu autogenous welds of both CC-GTAW and PC-GTAW first solidified as d ferrite near the fusion line of the weld as the composition allows for peritectic stiffness, followed by the solid phase of eutectic single austenite, characterized by a cellular structure. Metallographically difficult to separate the peritectic and eutectic ferrite phase is maintained within the intercellular boundaries of the autogenous weld, as the conversion of solid delta ferrite to austenite is incomplete due to separation. In pulsed current mode the surface of the melted liquid does not cool sufficiently in the background current, thus improving the cooling rate and welding of the welding metal. The current pulsing phenomenon is found to be beneficial in reducing the percentage of eutectic film separation in the intercellular and refractory filters in the welded GTAW joints of Super 304HCu austenitic stainless steel. The PC-GTAW joint showed higher tensile strength and elongation values than the CC-GTAW joint. However, the failure was found in the welding joint in both cases, indicating that no significant improvement was achieved in terms of strength by PC-GTAW compared to CCGTAW joints. Although PC-GTAW offers Super 304HCu austenitic stainless-steel joints with better properties than CCGTAW joints. GTA welding Super 304HCu in autogenous mode cannot avoid harmful alloy disintegration and produce weld joints with the required properties for high temperature inserts in USC boilers. In the case of Super 304HCu austenitic stainless-steel welding, it is recommended to use more powerful processes, as cooler levels higher than PC-GTAW can be achieved to avoid separation. The significant difference between the two outcomes further enhances the robustness and efficiency of using PCGTAW instead of CCGTAW pipe joints. The weld center and HAZ of PCGTAW joint displayed higher hardness than CCGTAW joint.

OTHER WORK AND EXPENSES

Other Work

Other work included the preparation of different samples and learning to manoeuvre different equipments. One such work was mount preparation for optical microscopy. The following figures 7.1 to 7.3 shows the mounds before polishing.

Fig 7.1 ORIGINAL SAMPLE

Fig 7.2 CCGTAW SAMPLE

Fig 7.3: PCGGTAW SAMPLE

All the three samples (No. 3) were mounted and then polished in the single disc polishing machine available at SRMIST-KTR (Figure 7.4).
Technical Specifications:
Speed: 1500 RPM
Disc Diameter: 210 mm
Polishing Material: Velvet Cloth 260 mm Diameter
Power: Single Phase Motor ½ HP

e-ISSN: 2250-0758 | p-ISSN: 2394-6962
Volume-12, Issue-4 (August 2022)
https://doi.org/10.31033/ijemr.12.4.27

Fig 7.4 SINGLE DISC POLISHING MACHINE


Fig 7.6 POLISHING OTHER SAMPLE


Fig 7.5 POLISHING

Figure 7.5 and 7.6 depicts the mound polishing using the equipment and abrasive agent. Next the samples were washed and dried. Figures 7.7 to 7.9 shows the samples after polishing. After this they were etched using a prepared sample of 3-parts hydrochloric acid and 1-part nitric acid.

Fig 7.7 ORIGINAL SAMPLE


Fig 7.8 CCGTAW SAMPLE


Fig 7.9: PCGGTAW SAMPLE

Using the optical microscope (figure 7.10) the microstructure analysis was carried out and the results were obtained.

e-ISSN: 2250-0758 | p-ISSN: 2394-6962
Volume-12, Issue-4 (August 2022)
https://doi.org/10.31033/ijemr.12.4.27

Fig 7.10 OPTICAL MICROSCOPE

Tensile test was carried out in VIT Chennai using the setup shown in figure 7.11.

Fig 7.11 TENSILE TEST SETUP

X-Ray Diffraction test was carried out in the X-Ray Diffractometer shown in figure 7.12.

Fig 7.12 X-Ray DIFFRACTOMETER

e-ISSN: 2250-0758 | p-ISSN: 2394-6962
Volume-12, Issue-4 (August 2022)
https://doi.org/10.31033/ijemr.12.4.27

Expenses

Expenses of the total project included buying of the material, preparation of the samples to all the tests conducted. The bifurcation of the entire project budget is provided as follows:

1.) ACQUIRING THE MATERIAL: Rs. 2500/- PER PERSON
= 2500 x 2 = Rs. 5000/-
2.) TIG (GTAW) WELDING: Rs. 100/- EACH PAIR
= 100 x 4 = Rs. 400/-
3.) SAMPLE PREPARATION: Rs. 1600/- PER SET
= 1600 x 3 = Rs. 4800/-
4.) TENSILE TEST: Rs. 450/- PER SAMPLE
= 450 x 3 = Rs. 1350/-
5.) MICROSTRUCTURE TEST: Rs. 250/- PER SAMPLE
= 250 x 3 = Rs. 750/-
6.) MICROHARDNESS TEST: Rs. 200/- PER SAMPLE
= 200 x 3 = Rs. 600/-
7.) XRD TEST: Rs. 150/- EACH SAMPLE
= 150 x 3 = Rs. 450/-
8.) TOTAL COST:
= 5000 + 400 + 4800 + 1350 + 750 + 600 + 450 = Rs. 13350/-

FUTURE ENHANCEMENTS

The weld joint is one of the weakest areas in a fabricated component. Therefore, it is necessary to consider the characteristics of the weld material to avoid failures. Weldability is usually characterized by resistance to hot cracking and the mechanical properties of the weld joints. To get more accurate results greater number of pipes of different diameters are needed and conducting CFD Simulations with hot steam to determine most efficient changes in material properties and dimensional aspects. The improvement of oxidation resistance could be attributed to the fact that the shot peening process produced a surface layer of ultra-fine grains with plenty of grain boundaries, sub-grain boundaries and dislocations, which enhanced the diffusion of Cr to form a layer of high density of Cr-rich oxides on the surface. Introducing advanced filler materials with the pulsating current gas tungsten arc welding will further enhance the desired results. Conducting Electron Back Scatter Diffraction will provide us with a detailed look into the structural and overall properties of the material and welds.

REFERENCES

[1] DataSheet DMV 304HCu – MANNESMANN STAINLESS TUBES
[2] A Balamurugan, M Mohan, E Venkatesan, T Ramkumar - Mechanical properties and microstructure analysis of super304 HCu joints using friction welding
[3] Viswanathan, R. and Bakker, W.T. - “Materials for ultra-supercritical fossil power plants”
[4] Kumar, S. and Shahi, A.S. - “Effect of heat input on the microstructure and mechanical properties of gas tungsten arc welded AISI 304 stainless steel joints”
[5] Khan, M.A., Sundarrajan, S. and Natarajan, S - “Hot corrosion behaviour of super 304H for marine applications at elevated temperatures”
[6] Yang, H.C., Peng, F.F., Miao, X.L. and Yang, X. - “Investigation of the aging behavior on boiler steel tube Super304H”
[7] Reddy, A.A., Guha, B. and Achar, D.R.G. - “Finite element modelling of three-dimensional transient heat transfer in stainless steel (304) pulsed GTA weldments”
Folkhard, E. - “Welding Metallurgy of Stainless Steels”
[8] TOHYAMA, A.; HAYAKAWA, H.; MINAMI, Y. – “Development of high strength steel boiler tube”
SAWARAGI, Y.; OGAWA, K.; KATO, S.; NATORI, A.;
[9] HIRANO, S. – “Development of the economical 18-8 stainless steel (SUPER 304H) having high elevated temperature strength for fossil fired boilers”
[10] Wei, Y., Xu, Y., Dong, Z. and Zhan, X. - “Three-dimensional Monte Carlo simulation of discontinuous grain growth in HAZ of stainless steel during GTAW process”